Materials Today Bio 8 (2020) 100079

Contents lists available at ScienceDirect

Materials Today Bio

journal homepage: www.journals.elsevier.com/materials-today-bio

Enzyme-mediated one-pot synthesis of hydrogel with the polyphenol cross-linker for skin regeneration

B.S. Kim [a,e], S.-H. Kim [a,b,c,e], K. Kim [a], Y.-H. An [b], K.-H. So [b], B.-G. Kim [a,b,d], N.S. Hwang [a,b,d,*]

[a] Interdisciplinary Program in Bioengineering, Seoul National University, Republic of Korea
[b] School of Chemical and Biological Engineering, Institute of Chemical Processes, Seoul National University, Republic of Korea
[c] John A. Paulson School of Engineering and Applied Sciences, Harvard University, Cambridge, MA, USA
[d] Bio-MAX Institute, Institute of Bio-Engineering, Seoul National University, Republic of Korea

ARTICLE INFO

Keywords:
Epigallocatechin gallate (EGCG)
Hydrogels
Chitosan
Anti-inflammatory
Wound healing

ABSTRACT

Polyphenols can trigger immunity that activates intracellular anti-inflammatory signaling and prevents external infections. In this study, we report the fabrication of chitosan-based hydrogels with epigallocatechin gallate (EGCG) using enzyme-mediated one-pot synthesis. The tyrosinase-mediated oxidative reaction of the phenolic rings of EGCG with the primary amines on chitosan results in stable EGCG-chitosan hydrogels. The EGCG concentrations contributed to the cross-linking density and physical properties of EGCG-chitosan hydrogels. Furthermore, EGCG-chitosan hydrogels maintained intrinsic properties such as antibacterial and antioxidant effects. When endotoxin-activated RAW 264.7 macrophage cells were cultured with EGCG-chitosan hydrogels, the hydrogels reduced the inflammatory response of the RAW 264.7 cells. Furthermore, subcutaneous implantation of EGCG-chitosan hydrogels reduced endogenous macrophage and monocyte activation. When the EGCG-chitosan hydrogels were applied to a full-skin defect wound, they facilitated skin regeneration. Our study demonstrates that the one-pot synthesized EGCG-chitosan hydrogels can be applied in broad tissue regeneration applications that require immune modulation.

1. Introduction

Polyphenols, one of the metabolic products in plant cells, have been widely established as useful molecules for immune-suppression and regenerative medicine applications [1]. The proposed mechanism of action of polyphenolic compounds is that they scavenge free radicals generated by immune cells and subsequently down-regulate tissue necrosis factors (TNFs) and interleukin-1 [2]. Among the various types of polyphenols, epigallocatechin gallate (EGCG) from green tea extract is known for its function as an antioxidant and anti-inflammatory [3–5]. EGCG has three phenolic ring structures. In the B and D rings, there is a 3, 4,5- trihydroxyphenyl moiety that acts as a therapeutic core by scavenging free radicals and substrates for biological molecules [7]. EGCG has been widely used to treat diseased tissue by mitigating a reactive oxygen species and regulating inflammatory cytokines [8,9]. Previously, the direct conjugation method that incorporated phenolic compounds like EGCG into biopolymers such as chitosan, hyaluronic acid, and alginate had been developed to utilize EGCG for therapeutic agents [7, 10–12]. Our group has developed EGCG-incorporated hydrogels by coupling EGCG to the hyaluronic acids for tissue glue [7,10]. However, it is time-consuming owing to several essential steps which needed to purify organic solvents or bioreactive chemical remains in cross-linkable moiety modification procedures [11].

In our previous study, we elucidated that the tyrosinase from *Streptomyces avermitilis* (SA_Ty) has unusually higher enzymatic kinetic activity toward EGCG molecules as cross-linker in mild conditions [7]. Compared with other naturally existing tyrosinases, SA_Ty has unusual catalytic activity. In particular, SA_Ty lacks neighboring residues that sterically hinder enzymatic reactions with phenolic compounds. The oxidative reaction of EGCG with tyrosinase has a similar mechanism to that in mussel-inspired chemistry: i) the trihydroxy phenolic ring is oxidized immediately to form a quinone adduct and ii) the quinone adduct reacts with a primary amine, thiol, or imidazole through a Schiff-base reaction and Michael-type addition [7,10,13]. The enzymatic oxidative reaction occurred at a high rate under physiological conditions and has no cytotoxicity [7,13]. Once producing reactive quinones after

* Corresponding author.
E-mail address: nshwang@snu.ac.kr (N.S. Hwang).
[e] Beom Seok –Kim and Su-Hwan Kim contributed equally to this work.

https://doi.org/10.1016/j.mtbio.2020.100079
Received 10 July 2020; Received in revised form 9 September 2020; Accepted 12 September 2020
Available online 21 September 2020

enzymatic oxidation, the EGCG can make a covalent bond with a primary amine. We hypothesized that, with an enzymatic reaction, EGCG would form a hydrogel with biopolymers containing primary amines in a one-pot synthesis without any other organic synthetic processes. We expected that EGCG would act as both a cross-linker of the enzymatic reaction and a biofunctional factor for reducing inflammation.

In this study, we report the one-pot synthesis of EGCG-chitosan hydrogel via tyrosinase-mediated cross-linking. We used chitosan as a model biopolymer. Chitosan is a natural polymer that has abundant primary amine residues in the backbone structure [14,15]. When mixing EGCG molecules with chitosan solution, chitosan participated in the oxidative reaction and formed a hydrogel through enzyme-mediated cross-linking. After confirming the cross-linking mechanism by Fourier-transform infrared spectroscopy (FT-IR), we evaluated the physicochemical properties with varying EGCG concentrations. Then, we evaluated whether the inherent properties of EGCG, such as antioxidant, antibacterial, and anti-inflammatory activity, could maintain after cross-linking. Finally, EGCG-chitosan hydrogels were applied to treat full-skin defect mouse models, where they effectively augmented skin tissue regeneration.

2. Material and methods

2.1. Isolation of tyrosinase from Streptomyces avermitilis

Recombinant plasmids were constructed in a previous study [16]. SA_Ty was collected as previously described [13]. The concentration of enzymes was measured by bicinchoninic acid assay (BCA) (Thermo Fisher Scientific Inc., USA) following the manufacturer's instructions.

2.2. Fabrication of EGCG-chitosan hydrogels

Initially, 3% (w/v) glycol chitosan (Molecular Weight degree of polymerization > 400, 60% titration; Sigma Aldrich, USA) solution was prepared by dissolving 300 mg of glycol chitosan in 10 mL of distilled water. Then, the EGCG (LG Healthcare, Republic of Korea) monomers were dissolved in Dimethyl sulfoxide (purity ≥99.9%, anhydrous, Sigma Aldrich, USA) at 42 mM, 98 mM, and 154 mM. Three different concentrations of EGCG solutions were diluted in 3% (w/v) glycol chitosan solutions to 3 mM, 7 mM, and 11 mM, respectively. Then, the SA_Ty stock solution was added to 5 μM. Pre-gel solutions were cross-linked for 3 h. Cross-linking time was verified by tilting vials until the flow of solutions was not observed.

2.3. FT-IR analysis

To verify the cross-linking mechanism of the EGCG-chitosan hydrogel, we prepared hydrogels with different cross-linking times (0 h, 1 h, and 3 h). Samples were characterized by FT-IR (PerkinElmer Frontier). All samples were scanned 30 times with a resolution of 8 cm^{-1} and measured at wavenumbers ranging from 500 to 4000 cm^{-1}. Pristine chitosan was used as a control group.

2.4. Nuclear magnetic resonance spectroscopy analysis

The ^{1}H NMR spectrum was determined on an Avance III 400 Spectrometers (Bruker, Germany). Glycol chitosan and raw EGCG monomer were dissolved in D_2O (99.9 atom % D, Sigma Aldrich, USA) solution (1%, w/v). EGCG-chitosan hydrogel powder was prepared by grinding lyophilized cross-linked hydrogel (11 mM EGCG concentration) in a mortar. This hydrogel powder also dissolved in D_2O solution (1% w/v). All solutions transferred to NMR tube (Chemglass, USA) and analyzed.

2.5. Complex-dissociation calculation of hydrogel

Samples were soaked in two different solutions (1 M sodium chloride [Biograde Sigam Aldrich, USA], and 5% [w/v] Triton X-100 solution [average molecular weight: 80,000, Sigma Aldrich]) for 24 h at 37 °C, to dissociate the polymer complex formed by non-covalent bonds. Freeze-drying steps were performed for measuring the weight of the remaining polymer components after processing. Weight loss ratios were calculated by the following equations (w_c is weight of hydrogel after cross-linking, and w_d indicates weight of hydrogel after freeze drying.)

$$\text{Complex dissociation ratio} = (w_c - w_d)/w_d \quad (1)$$

2.6. Measurement of EGCG-releasing profile

EGCG-chitosan hydrogels were incubated in 40 mM tris buffer (pH 7.4), and supernatants were collected every day for two weeks. After that, 40 μL of collected samples were transferred into a 96-well plate and mixed with 40 μL of Folin & Ciocalteu's phenol reagent (Sigma Aldrich, USA). After 3 min, 120 μL of 10.75 wt% sodium carbonate (≥99.0% (calculated based on dry substance, Sigma Aldrich, USA) was added; it was then stored in the dark for 3 h. The absorbance of the final solution was measured at 760 nm. The amount of EGCG was determined by comparing the absorbance with a calibration curve developed from native polyphenol.

2.7. Measurement of quinone quantities in the fabrication system

3 mM, 7 mM, and 11 mM of EGCG solutions and same volume of enzyme-treated EGCG solutions (3 mM, 7 mM, and 11 mM) were prepared. 40 μL of collected samples were transferred into a 96-well plate and mixed with 40 μL of Folin & Ciocalteu's phenol reagent. After 3 min, 120 μL of 10.75 wt% sodium carbonate was added; it was then stored in the dark for 3 h. Absorbance was measured in a specific wavelength (760 nm). Quantities of molecules were speculated by standard curve of polyphenol. Oxidized EGCG molecular concentrations were calculated by following equations.

$$\text{Oxidzed EGCG concent} = (Abs.\ of\ Raw\ EGCG\ -\ Enzyme\ treated\ samples\ ) \quad (2)$$

2.8. Measurement of swelling ratios of hydrogel

To measure the swelling ratio, fully cross-linked and swollen hydrogels were weighed and then lyophilized. The swelling ratio of EGCG-chitosan hydrogels was calculated using the following equation (w_w= weight of hydrogel after swollen, w_d = weight of hydrogel after freeze-drying):

$$\text{Swelling ratio} = (w_w - w_d)/w_d \quad (3)$$

2.9. Scanning electron microscope analysis

To observe the internal structure of the hydrogel, lyophilized hydrogels were sliced horizontally to expose the internal structure. Then the samples were coated with platinum/palladium and observed with a JSM-7610F Scanning Electron Microscope (JEOL USA Inc., USA) at 10 μA and 10 kV.

2.10. Rheological and mechanical analysis of hydrogels

Rheological analysis of EGCG-chitosan was conducted at Anton Paar Korea Ltd. using a rheometer (MCR 302; measuring cell: P-PTD & H-PTD 200; measuring system: PP 25; Anton Paar, Austria). Hydrogels were fabricated using a Polydimethylsiloxane (PDMS) mold with an 8 mm diameter and 2 mm thickness. All experiments were conducted at 37 °C. A strain sweep test was performed. When the strain increases, the intersection point of G′ and G″ indicates the critical strain. A frequency sweep test was also performed. G′ and G″ were measured when the

frequency decreased from 100 Hz to 0.1 Hz. The Young's modulus was measured using a Universal Testing Machine (UTM, Shimadzu, EZ-sx). The hydrogel samples were pressed at a rate of 1 mm/min of probe speed using the UTM. The Young's modulus was calculated from a linear region of the stress–strain curve (5%–15% strain).

2.11. Antibacterial analysis of EGCG-chitosan hydrogels

Antibacterial functions of EGCG-chitosan hydrogels were conducted using two different bacterial species. To prepare lysogenic broth (LB) (Becton Dickinson) agar gel, 3 g of agarose, and 5 g of LB broth were dissolved in 200 mL of distilled water. After autoclaving, it was poured into a petri dish. A 200 μL of *Escherichia coli* (*E. Coli*) or *Staphylococcus aureus* (*S. Aureus*) suspension was transferred to the prepared agar gel. Hydrogels were placed on the agar gel and incubated for 9 h. Areas of bacterial inhibition zones were calculated with ImageJ software. Next, the hydrogels were detached from the LB agar plates and immersed in fresh LB broth. After 3 h incubation, the optical density at 600 nm of the solution was measured and quantified.

2.12. Radical scavenging assays

To quantify the radical scavenging rate of released EGCG, the EGCG-chitosan hydrogels were soaked in 40 mM tris (Sigma Aldrich, USA) buffer (pH 7.4) for 24 h. Then, 100 μL of solution from each sample was collected and mixed with 100 μL of 0.1 mM 2,2-diphenyl-1-picrylhydrazyl solution (Sigam Aldrich, USA). Next, all samples were incubated in a light-protected environment for 30 min. Absorbance was measured at 517 nm with UV spectroscopy (TECAN Infinite m200 Pro, Switzerland). The α-tocopherol solution (5 mg/mL) was prepared for the positive control group. Tris-HCl buffer (Sigma Aldrich, USA) solution was used as a blank sample.

$$\text{Percentage of scavenging radical} = (Abs.\ of\ blank - \frac{Abs.\ of\ sample}{Abs.of\ blank}) \times 100 \quad (4)$$

2.13. Cell viability and proliferation test

C2C12 cells were cultured in a 96-well cell culture plate at a concentration of 1 x 10^4 cells per well, with the medium composed of Dulbecco's Modified Eagle medium (DMEM, high glucose 4500 mg/mL, Gibco, USA) supplemented with 10% (v/v) fetal bovine serum (Gibco, USA), 1% (w/v) L-glutamine (Gibco, USA), and 1% (v/v) penicillin-streptomycin (10,000U/ml penicillin, 10,000 mg/mL streptomycin, Gibco, USA). To observe the biological effects of EGCGs released from EGCG hydrogel, we incubated EGCG-chitosan hydrogel in a cell culture medium for 24 h and collected the released EGCGs. Collected EGCGs were further exposed to C2C12 cell, and viability and proliferation were measured using the PrestoBlue Cell Viability Reagent (Thermo Fisher Scientific Inc., USA) for 3 days. Live/dead cell numbers and ratios were quantified from images obtained with EVOS Cell Imaging Systems (Thermo Fisher Scientific Inc.).

2.14. Anti-inflammatory analysis of EGCG-chitosan hydrogels

At first, the EGCG-chitosan hydrogel was immersed into the base medium (DMEM supplemented with 10% fetal bovine serum, L-glutamine 1%, penicillin-streptomycin 1%) for 24 h to dissolve EGCG which released from hydrogel, and the medium was collected. RAW 264.7 cells were cultured on 96-well cell culture plates (cell density: 1 x 10^4 cells/well) with the growth medium. After that, 100 ng/mL of lipopolysaccharide (from *E. coli*, Sigma Aldrich, USA) was added to each well. After 6 h of stimulation with Lipopolysaccharide (LPS), the collected EGCG-contained medium was applied for 24 h. The cell culture medium was collected and the amounts of TNF-α were quantified using a mouse TNF-alpha ELISA Complete Kit (KOMA biotech, Republic of Korea).

2.15. Subcutaneous implantation and application in a full-thickness wound model

All animal experiments were performed using protocols approved by the Seoul National University Institutional Animal Care and Use Committees (SNU-141229-3-9). EGCG, glycol chitosan, and SA_Ty solution (30 μL) were mixed and injected into subcutaneous tissue in the dorsal cavity of BALB/C mice (female; age: 8 weeks; weight: 20–25 g) using a 31G needle syringe (BD Ultra-Fine™, USA). The same volume of Phosphate bufferd saline (PBS, Gibco, USA) was applied as a control. Skin samples were collected after 3 d for immunofluorescence staining. For full-thickness wound models, a biopsy punch with a 6 mm diameter was utilized, and EGCG-chitosan hydrogels were applied, with PBS as a control. Wound closure ratios were calculated with ImageJ software. Samples were collected at day 3, day 6, and day 10 for tissue staining procedures.

2.16. Histological analysis

Collected skin samples were fixed in 4% paraformaldehyde (Duksan science, Republic of Korea) solution for 24 h and dehydrated in proper ethanol solutions for 5 min each (50%, 75%, and 100%). After embedding tissue samples in paraffin solution, the samples were prepared to 10 μm thickness. Sliced tissue samples were immersed in xylene solution and rehydrated with ethanol (100%, 75%, and 50%) for 5 min each. The samples were stained with hematoxylin (Sigma Aldrich, USA) for 1 min, rinsed in running tap water for 10 min, and then stained with eosin (Sigma Aldrich, USA) for 5 min. After washing the tissue sections with running tap water, they were dehydrated with 50%, 75%, and 100% ethanol solutions, then mounted with mount solution (Clear Mount TM, Invitrogen, Thermo Fisher Scientific Inc., USA).

2.17. Immunofluorescence staining

Immunofluorescence staining was performed to verify the immune suppressive effects of the hydrogel in samples obtained from *in vivo* experiments. Tissue sections were prepared in 10 μm of thickness with the same methods described in the Hematoxylin and Eosin (H&E) staining section. The tissue samples were deparaffinized in xylene for 5 min and rehydrated with ethanol solutions (100%, 70%, and 90%) for 5 min each. The tissue samples were incubated in PBS solutions (20 μg/mL of proteinase K [Thermo Fisher Scientific Inc., USA] and 0.1% of Triton X-100) for 1 h to perform antigen retrieval and the tissue permeabilization process. After that, the tissue samples were blocked with 1% Bovine Serum Albumin (BSA, Thermo Fisher Scientific Inc., USA) and 10% goat serum (ab7481, Abcam, UK) in PBS solution for 20 min to hinder nonspecific antibody conjugation. Next, the tissue samples were incubated with primary antibody Anti-Monocyte/Machropage Antibody (MOMA-2, ab33451, Abcam, UK) overnight at 4 °C and then with secondary antibody (Santa Cruz Biotechnology Inc., USA) for 2 h at room temperature. 4′,6-DiAmidino-2-PhenylIndoe (DAPI) staining was performed for counterstaining and included PBS wash with each step.

2.18. Statistical analysis

All data are expressed as mean and standard deviation. Statistical significance was evaluated by Student's t-test with $^*p < 0.05$, $^{**}p < 0.01$, or $^{***}p < 0.001$.

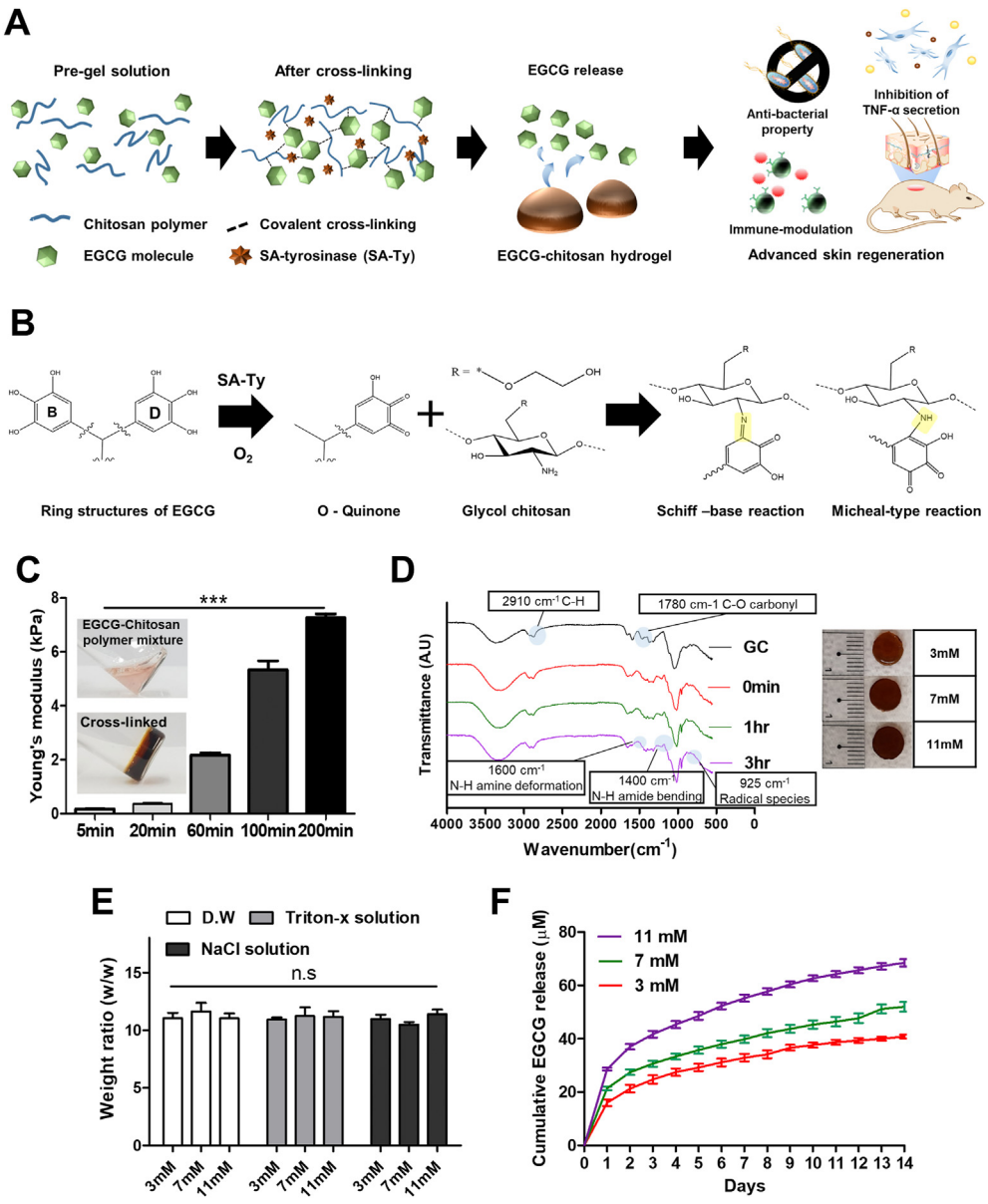

Fig. 1. EGCG-chitosan hydrogel cross-linking characteristics. (A) The schematic illustration of the fabrication of EGCG-chitosan hydrogel. (B) The cross-linking mechanism of EGCG-chitosan hydrogel. (C) Time-dependent cross-linking profiles and vial tilting tests for evaluation of hydrogel. (11 mM of EGCG was dissolved in glycol chitosan for tests) (D) Monitoring of EGCG-chitosan reaction by Fourier-transform infrared spectroscopy. (E) Quantification of complex dissociation of EGCG-chitosan hydrogel by Triton X-100 and sodium chloride. EGCG-chitosan hydrogel was not dissociated by Triton X-100 and sodium chloride which indicated hydrophobic interaction and hydrogen bond dissociation, respectively. (F) Release kinetics of EGCG from the hydrogel with different EGCG concentrations. EGCG, epigallocatechin gallate; SA_Ty, tyrosinase from *Streptomyces avermitilis*.

3. Results

3.1. Synthesis and characterization of enzyme-mediated EGCG-chitosan hydrogel

In this study, we report a simple enzymatically cross-linked EGCG-chitosan hydrogel for biomedical applications. A simple mixture of SA_Ty, EGCG, and glycol chitosan resulted in chitosan cross-linking by oxidized EGCG, forming a stable EGCG-chitosan hydrogel (Fig. 1A). As the EGCG can be oxidized by a tyrosinase reaction, the resultant molecule can make covalent bonds with primary amines in chitosan to form EGCG-chitosan hydrogels. The enzyme-mediated cross-linking were initiated after 5 min, hydrogels were fully cross-linked after 3 h (Fig. 1C). We confirmed the cross-linking mechanism by two different methods. At first, FT-IR was performed at various time points of oxidative reaction (Fig. 1D). As the radical species were produced by the quinone adduct, we speculated the location of peaks specifically indicating the formation of radical species in phenol (1780 cm^{-1}) and the product of phenoxyl radical–related coupling reaction (925 cm^{-1} and 2910 cm^{-1}). We also observed that the amide bond-related peaks (1400 cm^{-1} [N–H amide bending] and 1200–1300 cm^{-1} [C–N stretching]) were displayed and peaks increased in a reaction time-dependent manner. In addition, transmittance value decreased at 1600 cm^{-1} (N–H), which confirmed the reduction of amine residues in the chitosan polymer. It was demonstrated that tyrosinase could lead to oxidation of phenol to quinone, and oxidized EGCG would form covalent bonds with the amine groups of chitosan by Michael-type reactions [13]. The cross-linking mechanism of hydrogels was further explored by NMR spectroscopy analysis (Fig. S4). The multiple peaks in the range of 3.51–3.60 ppm are attributed to H-3 to H-8. The peaks at 2.55 ppm and 1.87 ppm correspond to H-2 and the residual $–CH_3$ [17]. The proton of EGCG appeared at 6.75, 6.29, and 5.25 ppm representing aromatic ring protons of the B, D, and A ring, respectively, and the proton of the C ring appeared at 2.6 ppm [18]. The successful hydrogel cross-linking was confirmed by disappeared proton peaks of EGCG and the appearance of new peaks at 2.50 and the range of the 3.3–3.55 NMR spectrum of EGCG-chitosan hydrogel (Fig S4 D).

We further performed a complex-dissociation analysis to see whether any of the non-covalent bonds contributed to the stability of the EGCG hydrogels [19]. Briefly, after cross-linking the hydrogel, we treated it with 1 M sodium chloride solution and 5% (w/v) Triton X-100 solution.

These solutions, in high concentration, can dissociate hydrogen bonding and hydrophobic interactions between molecules, respectively. After 24 h, samples were washed vigorously with distilled water three times and lyophilized. Then, we calculated the weight variance with the hydrogel and agents-treated hydrogel. The distilled water-treated hydrogel was used as a control. Complex-dissociation ratio analysis demonstrated that were no significant changes observed compared with the distilled water–treated control samples (Fig. 1E). This confirmed that covalent bonds between EGCG and glycol chitosan are the sole contributors to EGCG-chitosan hydrogel formation. Hydrogen bonding by the hydroxyl group in EGCG, and hydrophobic interaction of the phenolic ring in EGCG did not contribute to the hydrogel stability.

As a result of uncreated residues of EGCG in the EGCG-chitosan hydrogel mixtures, unbound EGCGs were released from the hydrogels. We quantified the EGCG released from EGCG-chitosan hydrogels (Fig. 1F). The unbound EGCG displayed an initial burst of release from the EGCG hydrogel. However, sustained release of EGCG over 2 weeks was observed in all EGCG-chitosan hydrogels. The amount of released EGCG was proportional to the incorporated EGCG concentration. The total amount of released EGCG molecules was about 27 ± 1.2 μM in the 3 mM group, 38 ± 3.4 μM in the 7 mM group, and 60 ± 2.5 μM in the 11 mM group.

3.2. Characterization of mechanical and rheological properties of EGCG-chitosan hydrogels

To verify the mechanical properties, we measured the Young's modulus, swelling ratio, and porosity of EGCG hydrogels (Fig. 2). We observed an EGCG concentration–dependent stiffness increase in the hydrogels, where the mechanical property of the hydrogels increased as we increased the EGCG concentrations (Fig. 2A). Furthermore, swelling ratios (q) of EGCG-chitosan hydrogels decreased as the EGCG concentrations were increased (Fig. 2B). These results demonstrated the increased cross-linking density as EGCGs participate as cross-linkers between glycol chitosan molecules. Furthermore, we examined the internal structure of EGCG-chitosan hydrogels after the hydrogels were lyophilized (Fig. 2C and D). The images obtained by scanning electron microscope analysis indicated that EGCG-chitosan with 11 mM EGCG displayed a denser pore-like structure within the hydrogels (Fig. 2C). When we quantified the average size of the pore-like structure within the hydrogels, it showed EGCG concentration–dependent decreasing tendency of pore sizes (207±19 μm for 3 mM, 95± 8.4 μm for 7 mM, and 66±7.5 μm for 11 mM). A 11 mM EGCG-chitosan resulted in the smallest pore size of 66 ± 7.5 μm. These analyses confirmed that EGCG participated as a cross-linker to bridge the chitosan backbone during hydrogel formation. Viscous and elastic properties of hydrogels were investigated by strain and frequency sweep tests. Storage modulus (G′) values were sustained in the frequency sweep test, and considerably smaller loss modulus (G″) data were also plotted; the G′ value has 100 times higher measurements than G″, and this result demonstrates the formation of the hydrogel in the investigated range (Fig. 2E). At a strain range of 80–120, crossover of G′ and G″ values occurred, revealing the sol–gel transition and structure deformation of hydrogels by inducing strain (Fig. 2F). We further confirmed the biocompatibility of EGCG. Cell cytotoxicity was not observed in EGCG-containing DMEM-treated samples (Fig. S1A). Proliferation ratios were also measured with PrestoBlue reagents and

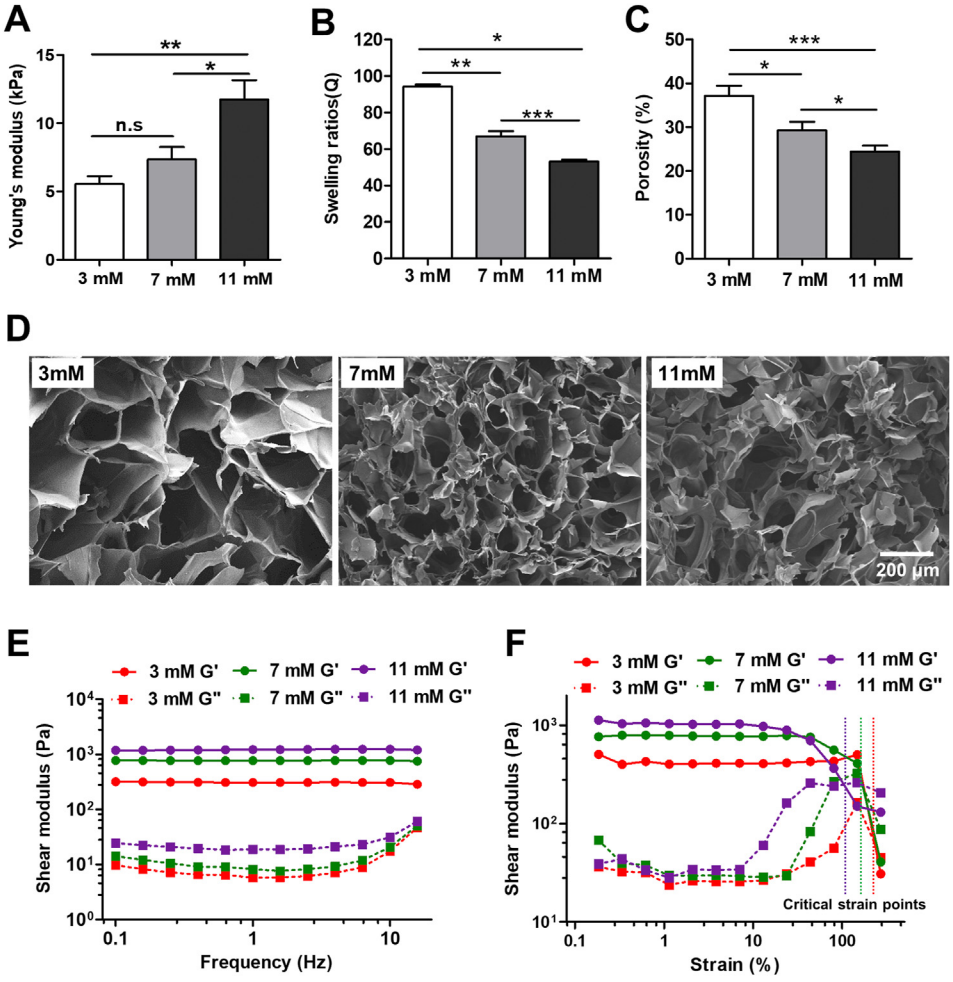

Fig. 2. Mechanical and rheological properties of EGCG-chitosan hydrogel. (A) The Young's modulus of hydrogel was quantified at different EGCG concentrations of hydrogel (3 mM, 7 mM, 11 mM). (B) Swelling ratios of each hydrogel were measured after 24h incubation in distilled water. (C) The pore density of the hydrogel was quantified. (D) SEM images of the porous structure of hydrogel. (E, F) Rheological evaluations of EGCG-chitosan hydrogel. Rheological properties of hydrogel were confirmed with frequency sweep and strain sweep tests. EGCG, epigallocatechin gallate.

found to increase by time elapsed with all group samples; there were no significant differences (Fig. S1B).

3.3. Antibacterial effect of EGCG-chitosan hydrogel

Antibacterial tests were performed with two different species of (*E. coli*, *S. aureus*) of bacteria. Hydrogel samples were placed on the surface of agar-bacterial plates where bacteria colonies had proliferated. After 24 h incubation, we quantified the antibacterial functions of the hydrogel samples by measuring the areas of bacterial inhibition zones. Bacterial colony-forming units were inhibited at hydrogel treated positions of the plates. Culture plates treated with hydrogels which contained 3 mM or 7 mM concentrations of EGCG had 0.42±0.01cm^2 and 0.47±0.03 cm^2 of bacterial inhibition zones each. 11 mM EGCG hydrogel samples resulted in 1.2±0.15 cm^2 of bacterial proliferation inhibited areas, which was two times higher than the other hydrogel samples (Fig. 3B). Antibacterial abilities were also quantified with optical density measuring (Fig. 3C). 11 mM EGCG hydrogel–treated samples showed the lowest bacteria proliferation in the bacteria culture medium, and 3 mM and 7 mM EGCG hydrogel–treated groups had no significant differences (Fig. 3C). Similarly, areas of the bacterial inhibition zone were 0.21± 0.06 cm^2 for 3 mM EGCG hydrogel, 0.22±0.03 cm^2 for 7 mM EGCG hydrogel, and 0.33±0.13 cm^2 for 11 mM EGCG hydrogel with *S. aureus* (Fig. 3D and E). EGCG-chitosan hydrogel with 11 mM EGCG showed the lowest bacteria proliferation of *S. aureus* (Fig. 3F). This result showed that the hydrogels we made had antibacterial abilities dependent on EGCG concentrations.

3.4. In vitro and in vivo anti-inflammatory activity of EGCG-chitosan hydrogel

We conducted *in vitro* tests to characterize TNF-α inhibition abilities induced by the anti-oxidative function of the EGCG molecules in hydrogel. Cytokine levels were varied by concentrations of EGCG in the cell culture medium (Fig. 4A). LPS-only treated groups had about 1000 pg/mL of TNF-α density in their medium, but by adding EGCG (3 mM, 7 mM, and 11 mM concentrations) to their culture conditions, TNF-α secretion level was decreased to 520 ±22.88pg/mL, 450±16.36 pg/mL, and 330±31.88 pg/mL, respectively, because of the anti-inflammatory functions of the polyphenols released from hydrogels. After quantifying the anti-inflammatory functions of the EGCG-chitosan hydrogel, polyphenol-only containing medium was treated with macrophage media without endotoxin (LPS) to determine the inflammatory responses of cells induced by EGCG molecules (Fig. 4B). EGCG-treated groups showed elevated TNF-α secretion levels in their EGCG-containing media versus the negative control, but the degree of TNF-α secretion was insignificant compared to the negative control. In addition, cytokine-release amounts were significantly lower than the samples with LPS stimulation. EGCG molecules did not evoke inflammatory responses in cellular environments but related to decreasing cytokines in particular conditions, stimulated by outside sources. In the diphenyl-1-picrylhydrazyl radical scavenging test, the samples which contain released EGCG from hydrogels had 37±1.88%, 52±3.13%, and 63±1.06% of radical scavenging abilities in accordance with their different EGCG concentrations (Fig. 4C). The 11 mM EGCG samples had equivalent antioxidant effects when compared with α-tocopherol solution (positive control) in the experiments.

We hypothesized that the EGCG components of the EGCG-chitosan hydrogel might affect tissue reconstruction with the possibility of inhibiting inflammation related to immune responses in wound defects. To verify the immunomodulatory functions of the hydrogel, we injected a pre-gel solution into the dorsal skin of mice. After 3 d, tissue samples were immunostained with the MOMA-2 antibody and DAPI reagents to

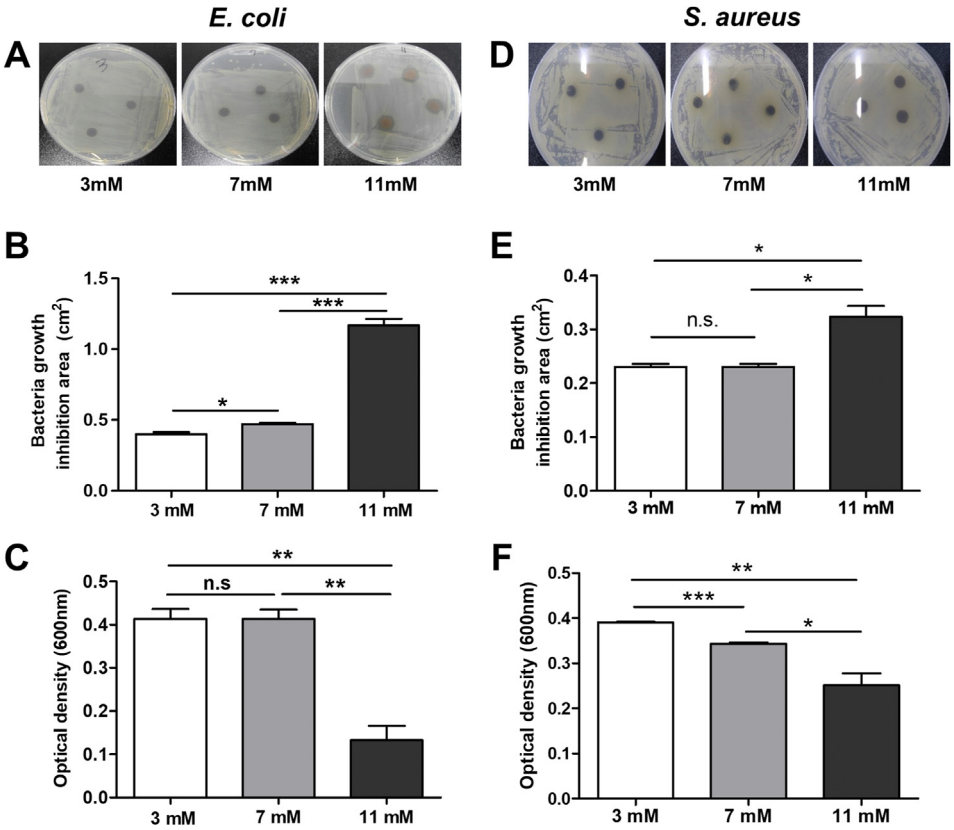

Fig. 3. Antibacterial abilities of EGCG-chitosan hydrogel were performed with two different kinds of bacteria (A, B, C): *E. coli*, (D, E, F): *S. aureus*. (A, D) Representative images of growth inhibition of bacteria on agar plates. (B, E) Antibacterial ability was quantified by measuring surface area of bacteria growth inhibited area. (C, F) Bacteria growth inhibition quantification with optical density at 600 nm. EGCG, epigallocatechin gallate.

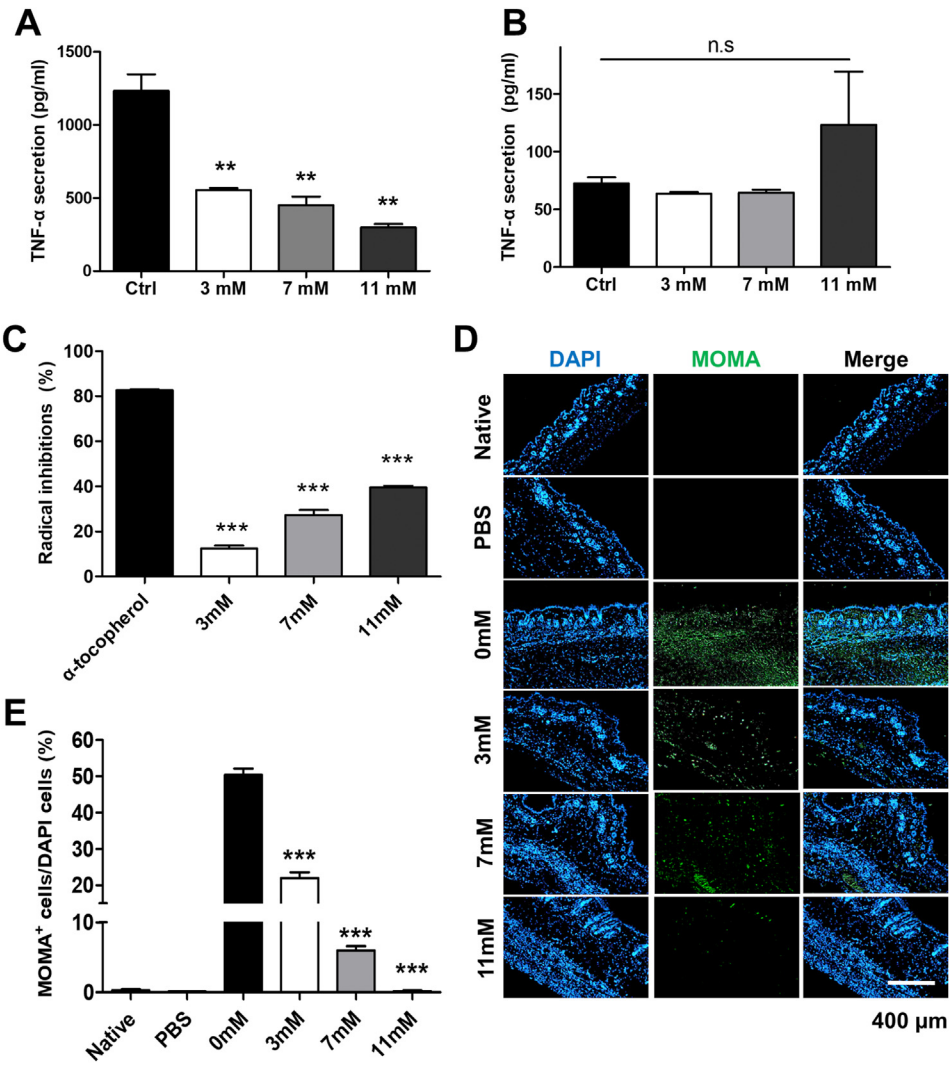

Fig. 4. Antioxidant, anti-inflammatory, and immune modulatory function of hydrogel. (A, B) Anti-inflammatory function characterization by measuring TNF-α cytokine release. (A) The RAW 264.7 cell culture with the EGCG-dissolved medium (with Lipopolysaccharide (LPS) stimulation). (B) The RAW 264.7 cell culture with EGCG-dissolved medium (without Lipopolysaccharide (LPS) stimulation). TNF-α release was quantified with ELISA kit. (C) Radical scavenging ability of hydrogel was quantified. 5 mg/mL of α-tocopherol solution was used as the control group. (D) Immunostaining of hydrogel injected skin tissues. The green and blue color represents immune cells (monocytes, macrophages) and cell nucleus, respectively. (E) Quantification of immune cell densities in tissues. (3 mM, 7 mM, 11 mM: EGCG concentrations in chitosan solution, 0 mM chitosan without EGCG, Phosphate bufferd saline (PBS), native: non-treated). (For interpretation of the references to color in this figure legend, the reader is referred to the Web version of this article.) EGCG, epigallocatechin gallate; TNF, tissue necrosis factor.

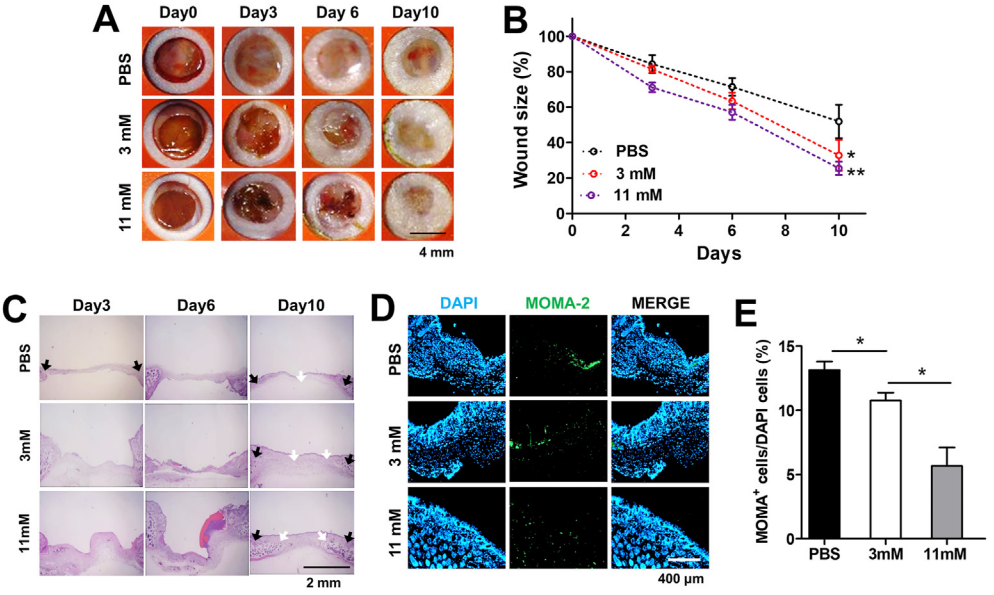

Fig. 5. *In vivo* mouse skin full defect model. (A) Representative images of wound closure on days 0, 3, 6 and 10. (B) Wound closure ratio were calculated. As increasing EGCG concentrations, wound closure process was accelerated. (C) Hematoxylin and Eosin (H&E) staining images of wound defects. Wound defect models treated with EGCG-chitosan hydrogels showed enhanced wound regeneration than control group. (Black arrow: periphery skin tissues, White arrow: regenerated skin tissues). Immunomodulatory function of EGCG-chitosan hydrogel (D, E). (D) Representative images of Anti-Monocyte/Machropage Antibody (MOMA-2) stained wound area. (E) Quantitative data of Anti-Monocyte/Machropage Antibody (MOMA-2) stained immune cells versus 4′,6-DiAmidino-2-PhenylIndoe (DAPI) stained tissues. EGCG, epigallocatechin gallate.

characterize MOMA-2–stained immune cells against DAPI backgrounds (Fig. 4D). Native tissues and the PBS-only treated group did not show acute immune responses compared with the EGCG-chitosan hydrogels. But in the chitosan-treated samples without EGCG, a large portion of immune cells were stained with antibodies because of immune responses. Immune cell densities were calculated by dividing the MOMA-2 stained cell fluorescence by the DAPI-stained fluorescence (Fig. 4E). By increasing the EGCG concentration, macrophage and monocyte cell populations were decreased in hydrogel intact tissues. Even the lowest concentration of EGCG, the 3 mM EGCG hydrogel group, showed dramatically decreased immune cell migrations in target tissues. The averages of quantified MOMA-2 staining fluorescence of samples were 22±4.2%%, 6±0.60%, and 0.21±0.18% in the experimental group samples (3 mM, 7 mM, and 11 mM EGCG hydrogel groups, respectively). This result demonstrated that EGCG molecules suppress immune cell responses in an *in vivo* model, and the strength of this immunomodulatory function is regulated by the EGCG concentrations in the hydrogel. Fig. 4 showed also the relation of anti-inflammatory functions and immune responses in cellular environments, and the potent abilities of EGCG molecules in hydrogels were maintained even after the hydrogel fabrication process and implantation in an animal model.

3.5. *In vivo mouse skin full defect model*

An *in vivo* mouse model was made by punching the dorsal skin with a 6 mm diameter biopsy punch. We implanted four different samples into the skin wound: i) PBS (negative control), ii) EGCG-chitosan hydrogels (3 mM or 11 mM concentration of EGCG in glycol chitosan 3% [w/v]). Wound defects were imaged before tissue collection at days 0, 3, 6, and 10 (Fig. 5A). Wound closure ratios of the samples were calculated using the areas of the initial wound defects and the time-dependent decreased wound areas. The 3 mM EGCG hydrogel treated groups had advantages over the PBS-treated group, and the 11 mM EGCG hydrogel–applied group showed faster healing ability than other groups (Fig. 5B). Histological analysis demonstrated that the PBS-treated group resulted in a thin granulation formation and lacked significant tissue regeneration. However, the 11 mM EGCG hydrogel–treated samples showed enhanced tissue reconstruction in wound sites. In particular, a representative image of H&E stained 11 mM EGCG samples exhibited many more portions of hair follicle and gland regeneration than the other group samples (Fig. 5C). Immunomodulation ability of hydrogels was characterized by the MOMA-2 antibody staining of wound defects (Fig. 5D). PBS-treated samples, without EGCG, showed an increased amount of the MOMA-2–positive cell level comparatively, and MOMA-2–positive immune cell levels were reduced with increasing EGCG molecules in the EGCG-chitosan hydrogels (Fig. 5E). These results demonstrate that the EGCG molecule is a highly efficient immune reaction modulator in a full-thickness wound model that can inhibit immune cell responses in wound sites.

4. Discussion

This study describes the characterization and biological evaluation of EGCG-chitosan hydrogels as a novel scaffold system for wound regeneration. Previously, a variety of adhesive hydrogels based on mussel-inspired chemistry were fabricated with antibacterial, conductive, or drug-releasing properties for enhanced wound repair [20–25]. Similarly, we utilized oxidation of phenolic moieties as a cross-linker to fabricate chitosan-based hydrogel in a one-pot system. In particular, we utilized EGCG as a source for the phenolic compounds as the efficacies of EGCG in a variety of human disease models are well documented [26–28]. Even though the free form of EGCG has been investigated for clinical proof of concepts, there has not been a report of EGCG as a simple cross-linker for a chitosan-based hydrogel. In this study, we report that a glycol chitosan-based hydrogel can be fabricated by mixing SA_Ty enzyme, EGCG, and glycol chitosan without any other chemical modifications. An EGCG-chitosan hydrogel has several advantages over other known natural polysaccharides. Chitosan's propensity to inhibit bacterial growth makes it an ideal component for a hydrogel-based patch for wound healing applications. In addition to chitosan, the polymers have amine groups that can form Michael-type addition with quinone groups on EGCG as the result of tyrosinase activation. Furthermore, unreacted EGCG molecules can be retained within EGCG-chitosan hydrogel and be released from the hydrogel in a steady and sustained fashion.

In our study, complete cross-linking took 3 h. A measurable increase in mechanical properties of the hydrogels was confirmed after 5min of reaction. In addition, there was an increase in mechanical property as time elapsed until 3 h (Fig. 1C). Even though EGCG works as a natural inhibitor of tyrosinase enzyme, we propose that tyrosinase induced oxidation of EGCG molecules that resulted in reactive quinones [29]. Reactive quinone formation from oxidized EGCGs attributed to amide bond formations with glycol chitosan (Fig. 1B, Fig. S2). For analyzing accurate bonding formation, the covalent incorporation of EGCG into glycol chitosan polymers was confirmed by FT-IR analysis (Fig. 1D). Because chitosan groups have amine groups, C–N bonds were formed with quinone groups by Michael-type reaction [13,30]. In addition, we confirmed the covalent linkage and stable structure of hydrogel by exposing it to disruption solutions. The disruption solutions, high concentrations of sodium chloride and Triton X-100, can break ionic or hydrophobic interactions and linkages between molecules [19]. Cross-linked EGCG-chitosan hydrogel immersed in sodium chloride and Triton X-100 solutions for 24 h did not cause any weight loss or structural changes in the hydrogel (Fig. 1E). These results verified formation of covalent cross-linking in hydrogel networks and participation of EGCGs as cross-linkers in hydrogel, conjugating to amine groups in chitosan polymers. In addition, for controlling the EGCG incorporation in hydrogel solutions, stiffness and swelling ratios of the hydrogels were managed by EGCG concentrations in hydrogel solutions (Fig. 2A and B). The mechanical properties of hydrogel were gradually managed with EGCG concentration and linkage properties in reaction processes. This data prove that EGCG molecules successfully reacted as cross-linkers in an enzyme-mediated hydrogel fabrication system.

Interestingly, we observed that not all EGCGs participated in hydrogel cross-linking procedures (Fig. S2, Fig. 1F). Oxidized EGCG by tyrosinase can be coupled with primary amines on the glycol chitosan. However, upon completion of hydrogel formation, unconjugated or unreacted EGCGs may be retained within the hydrogel structure [31,32]. These EGCGs may be entrapped within a cross-linked hydrogel network and are prone to sustained release from the hydrogel (via diffusion). Additional analysis of released EGCGs in respect to the total EGCGs in one-pot synthesis showed that 9.1±0.81% of EGCGs remained unconjugated (Fig. S5). Therefore, unreacted EGCGs released from hydrogels contributed as a biological drug in our *in vitro* and *in vivo* experiments. When we measured the release profiles of EGCG molecules for 14 d, EGCGs were released in a steady and sustained manner. Saturated EGCG contents released from 3 mM, 7 mM, and 11 mM EGCG-chitosan hydrogel samples were increased with concentration of molecules in it (Fig. 1F). EGCG molecules in extremely high concentrations (1 mg/mL) hindered cell proliferation in cell culture environments [8]. However, EGCG concentration–dependent cross-linked hydrogel managed the release of proper amounts of EGCG, less than 1 mg/mL, and showed advanced biocompatibility of the fabricated hydrogel (Fig. S1). This releasing behavior is very relevant in the topical application of EGCG-chitosan hydrogels and can allow sustained delivery of proper anti-inflammatory EGCG molecules in dermatological applications, as demonstrated.

In the wound healing process, the protection of the wound site from infection is an important issue [33,34]. In this study, we confirmed that EGCG-chitosan hydrogels exhibited antimicrobial functions (Fig. 3). The antibacterial properties of EGCG-chitosan increased along with the dissolved EGCG concentrations in the hydrogel (Fig. 3A and D). Purportedly, charged chitosan polymers have been shown to destroy negatively charged bacterial cell membranes, and EGCG molecules have been used

as antibacterial materials by interacting with surface proteins [35,36]. The antibacterial properties of the EGCG-chitosan hydrogel were effective with chitosan and EGCG, but higher concentration of EGCG prevents microbial attachment and lysis more efficiently (Fig. 3C and F).

EGCG molecules are known as biochemical effectors which reduce lipid peroxidation and radical formation and ameliorate pro-inflammatory cytokine release [37]. Anti-inflammatory effects of polyphenols were studied previously by inhibiting cytokine secretions in immune cells [38]. One of the cytokines, TNF-α, is a representative factor of inflammation responses in microenvironments [39]. Unoxidized EGCGs suppressed LPS-induced inflammatory activation (Fig. S3). Furthermore, EGCGs which released from the hydrogel perform similar anti-inflammatory actions with unoxidized EGCG (Fig. 4A). These results demonstrated that EGCG-chitosan hydrogel released unreacted EGCG, which maintained their original function even after oxidation process (Fig. S3, Fig. 4A). Released EGCG from EGCG-chitosan hydrogels also could hinder cytokine secretion in cell environments (Fig. 4A) and performed as a radical scavenger *in vitro* (Fig. 4C). These results demonstrated that polyphenols maintained their own functions after the enzymatic oxidation process which induced during the gel cross-linking mechanism. In addition, the functionality of EGCG is increased with relative EGCG concentration in hydrogel, and this profile proves that the EGCG-chitosan hydrogel platform, as a drug carrier, can be used for biomedical applications which need inhibitory control of inflammatory responses in a sustained manner (Figs. 1F and 4A). In a previous study, there was evidence of the anti-inflammatory functions of polyphenols in the inhibition of inflammatory stress and unexpected immune responses of cells, which release pro-inflammatory cytokines [40]. Accordingly, the EGCG-chitosan hydrogel prevented immune cell aggregation upon subcutaneous implantation. We observed that immune cell recruitment was obvious at low EGCG concentration (Fig. 4D). It seems that EGCG molecules decrease cytokine releasing and immune cell densities selectively in tissues by anti-inflammatory–relative immune inhibition effects (Fig. 4E).

The advanced wound care study has shown that application of high concentrations of polyphenols to wound repair has antibacterial and cytokine-release inhibition effects [41,42]. In addition, the chitosan polymer, incorporated as a hydrogel backbone, has been applied for wound care with antibacterial effects and exhibited biocompatibility [43]. Thus, in this paper, we investigated the regenerative ability of an EGCG-chitosan hydrogel using an animal wound defect model (Fig. 5). Wound regeneration ability improved more when EGCG molecules were incorporated into the chitosan hydrogel (Fig. 5A). The wound healing, soft tissue reconstruction, and ability of chitosan hydrogel was further enhanced with the addition of EGCG molecules (Fig. 5B). The results proved EGCG-chitosan conjugates performed advanced wound regeneration in an EGCG concentration–dependent manner. For moderate tissue reconstruction, immune cell recruitment was necessary in the early phase of regeneration process. However, overexpression of free radicals and cytokines in microenvironments which upregulate immune cell and pro-inflammatory mediators in injury [44] hamper tissue reconstruction [45]. For this reason, decreasing inflammatory responses has been used as one of the promising approaches for wound regeneration [46,47]. In the case of the PBS group, immune cells were highly infiltrated into the wound area (Fig. 5D). However, as EGCG-chitosan hydrogels were applied to skin wounds, immune cell populations gradually declined (Fig. 5E). In addition, wound regeneration was accelerated (Fig. 5B). From what was described earlier, we concluded that the EGCG-chitosan hydrogel fabrication system successfully maintained the inherent characteristics of the raw materials which enzymatically reacted in the synthesis process. Without denaturing the molecules used as cross-linkers in the enzymatic hydrogel fabrication platform, the hydrogel also demonstrated a controllable ability to release the utilized EGCG molecules *in vivo* (Fig. 5A). The stable reaction of EGCG and dose-dependent immune cell level modulation induced direct wound regeneration in target tissues with a gradual release profile of EGCG from the hydrogel.

In conclusion, by implementing EGCG as a cross-linker and biofunctional molecule with enzymatic reactions, we have developed one-pot synthesis of an EGCG-chitosan hydrogel to regenerate skin wounds. We confirmed that the radical-scavenging and anti-inflammatory functions of EGCG were highly suppressing *in vitro* and *in vivo* immune reactions (Figs. 4A and 5D). In addition, thanks to glycol chitosan and EGCG, the EGCG-chitosan hydrogel can inhibit different species of bacterial growth (Fig. 3). Finally, we applied EGCG-chitosan hydrogels to a mouse full-thickness skin defect model because the EGCG scavenged free radicals and suppressed immune reaction in the wound site; the EGCG-chitosan hydrogel can accelerate tissue remodeling process and implement wound healing without side effects (Fig. 5A). This manuscript demonstrated that one-pot synthesized EGCG-chitosan hydrogels could be applied for the accelerated wound treatment by modulating immune reactions. In addition, the one-pot synthesis system can be applied to incorporate other bioactive molecules or growth factors with tyramine or phenolic moieties to modulate the cell behavior or control stem cell differentiation [48–51].

Credit author statement

Beom Seok Kim: Methodology, Investigation, Writing - original draft, Writing-revision, Su-Hwan Kim: Methodology, Conceptualization, Writing - original draft, Writing-revision, Kyungmin Kim: Methodology, Writing - original draft, Young-Hyeon An: Data curation, Kyung-Ha So: Data curation, Byung-Gee Kim: Reviewing, Nathaniel S. Hwang: Conceptualization, Writing - original draft, Writing-revision.

Declaration of competing interest

The authors declare that they have no known competing financial interests or personal relationships that could have appeared to influence the work reported in this paper.

Acknowledgments

This work was financially supported by the Ministry of Science and ICT Future planning (NRF-2016R1E1A1A01943393, NRF-2017M3A9C6031786, NRF-2019M3A9G1023840, NRF-2019R1I1A1A01059554, and NRF-2019M3A9H1103786). The Institute of Engineering Research at Seoul National University provided research facilities for this work.

Appendix ASupplementary data

Supplementary data to this article can be found online at https://doi.org/10.1016/j.mtbio.2020.100079.

References

[1] M. Daglia, Polyphenols as antimicrobial agents, Curr. Opin. Biotechnol. 23 (2) (2012) 174–181.
[2] M. Larrosa, C. Luceri, E. Vivoli, C. Pagliuca, M. Lodovici, G. Moneti, P. Dolara, Polyphenol metabolites from colonic microbiota exert anti-inflammatory activity on different inflammation models, Mol. Nutr. Food Res. 53 (8) (2009) 1044–1054.
[3] H. Xu, T. Liu, J. Li, J. Xu, F. Chen, L. Hu, B. Zhang, C. Zi, X. Wang, J. Sheng, Oxidation derivative of (-)-epigallocatechin-3-gallate (EGCG) inhibits RANKL-induced osteoclastogenesis by suppressing RANK signaling pathways in RAW 264.7 cells, Biomed. Pharmacother. 118 (2019) 109237.
[4] S. Torabian, E. Haddad, S. Rajaram, J. Banta, J. Sabate, Acute effect of nut consumption on plasma total polyphenols, antioxidant capacity and lipid peroxidation, J. Hum. Nutr. Diet. 22 (1) (2009) 64–71.
[5] J.A. Nichols, S.K. Katiyar, Skin photoprotection by natural polyphenols: anti-inflammatory, antioxidant and DNA repair mechanisms, Archives. Dermatological Res 302 (2) (2010) 71–83.
[7] S.-H. Kim, K. Kim, B.S. Kim, Y.-H. An, U.-J. Lee, S.-H. Lee, S.L. Kim, B.-G. Kim, N.S. Hwang, Fabrication of Polyphenol-Incorporated Anti-inflammatory Hydrogel via High-Affinity Enzymatic Crosslinking for Wet Tissue Adhesion, Biomaterials, 2020, p. 119905.

[8] H. Kim, T. Kawazoe, D.W. Han, K. Matsumara, S. Suzuki, S. Tsutsumi, S.H. Hyon, Enhanced wound healing by an epigallocatechin gallate-incorporated collagen sponge in diabetic mice, Wound Repair Regen. 16 (5) (2008) 714–720.
[9] J. Thawonsuwan, V. Kiron, S. Satoh, A. Panigrahi, V. Verlhac, Epigallocatechin-3-gallate (EGCG) affects the antioxidant and immune defense of the rainbow trout, Oncorhynchus mykiss, Fish Physiol. Biochem. 36 (3) (2010) 687–697.
[10] Y.-H. An, H.D. Kim, K. Kim, S.-H. Lee, H.-G. Yim, B.-G. Kim, N.S. Hwang, Enzyme-mediated tissue adhesive hydrogels for meniscus repair, Int. J. Biol. Macromol. 110 (2018) 479–487.
[11] U.G. Spizzirri, F. Iemma, F. Puoci, G. Cirillo, M. Curcio, O.I. Parisi, N. Picci, Synthesis of antioxidant polymers by grafting of gallic acid and catechin on gelatin, Biomacromolecules 10 (7) (2009) 1923–1930.
[12] L. Cheng, Y. Wang, G. Sun, S. Wen, L. Deng, H. Zhang, W. Cui, Hydration-enhanced lubricating electrospun nanofibrous membranes prevent tissue adhesion, Research 2020 (2020) 4907185.
[13] S.-H. Kim, S.-H. Lee, J.-E. Lee, S.J. Park, K. Kim, I.S. Kim, Y.-S. Lee, N.S. Hwang, B.-G. Kim, Tissue adhesive, rapid forming, and sprayable ECM hydrogel via recombinant tyrosinase crosslinking, Biomaterials 178 (2018) 401–412.
[14] A.S. Hoffman, Hydrogels for biomedical applications, Adv. Drug Deliv. Rev. 64 (2012) 18–23.
[15] F.-L. Mi, H.-W. Sung, S.-S. Shyu, C.-C. Su, C.-K. Peng, Synthesis and characterization of biodegradable TPP/genipin co-crosslinked chitosan gel beads, Polymer 44 (21) (2003) 6521–6530.
[16] S.H. Lee, K. Baek, J.E. Lee, B.G. Kim, Using tyrosinase as a monophenol monooxygenase: a combined strategy for effective inhibition of melanin formation, Biotechnol. Bioeng. 113 (4) (2016) 735–743.
[17] A. Yu, H. Shi, H. Liu, Z. Bao, M. Dai, D. Lin, D. Lin, X. Xu, X. Li, Y. Wang, Mucoadhesive dexamethasone-glycol chitosan nanoparticles for ophthalmic drug delivery, Int. J. Pharm. 575 (2020) 118943.
[18] N. Fu, Z. Zhou, T.B. Jones, T.T. Tan, W.D. Wu, S.X. Lin, X.D. Chen, P.P. Chan, Production of monodisperse epigallocatechin gallate (EGCG) microparticles by spray drying for high antioxidant activity retention, Int. J. Pharm. 413 (1–2) (2011) 155–166.
[19] J.E. Chung, S. Tan, S.J. Gao, N. Yongvongsoontorn, S.H. Kim, J.H. Lee, H.S. Choi, H. Yano, L. Zhuo, M. Kurisawa, Self-assembled micellar nanocomplexes comprising green tea catechin derivatives and protein drugs for cancer therapy, Nat. Nanotechnol. 9 (11) (2014) 907.
[20] Y. Liang, X. Zhao, T. Hu, B. Chen, Z. Yin, P.X. Ma, B.J.S. Guo, Adhesive Hemostatic Conducting Injectable Composite Hydrogels with Sustained Drug Release and Photothermal Antibacterial Activity to Promote Full-thickness Skin Regeneration during Wound Healing, vol. 15, 2019, p. 1900046, 12.
[21] J. Qu, X. Zhao, Y. Liang, T. Zhang, P.X. Ma, B.J.B. Guo, Antibacterial adhesive injectable hydrogels with rapid self-healing, extensibility and compressibility as wound dressing for joints skin wound healing, Biomaterials 183 (2018) 185–199.
[22] X. Zhao, H. Wu, B. Guo, R. Dong, Y. Qiu, P.X.J.B. Ma, Antibacterial anti-oxidant electroactive injectable hydrogel as self-healing wound dressing with hemostasis and adhesiveness for cutaneous wound, healing 122 (2017) 34–47.
[23] J. He, M. Shi, Y. Liang, B.J.C.E.J. Guo, Conductive Adhesive Self-Healing Nanocomposite Hydrogel Wound Dressing for Photothermal Therapy of Infected Full-Thickness Skin Wounds, 2020, p. 124888.
[24] X. Zhao, B. Guo, H. Wu, Y. Liang, P.X.J.N.c. Ma, Injectable Antibacterial Conductive Nanocomposite Cryogels with Rapid Shape Recovery for Noncompressible Hemorrhage and Wound Healing, vol. 9, 2018, pp. 1–17, 1.
[25] Y. Liang, B. Chen, M. Li, J. He, Z. Yin, B.J.B. Guo, Injectable Antimicrobial Conductive Hydrogels for Wound Disinfection and Infectious Wound Healing, vol. 21, 2020, pp. 1841–1852, 5.
[26] A. Cano, M. Ettcheto, J.-H. Chang, E. Barroso, M. Espina, B.A. Kühne, M. Barenys, C. Auladell, J. Folch, E.B. Souto, Dual-drug loaded nanoparticles of Epigallocatechin-3-gallate (EGCG)/Ascorbic acid enhance therapeutic efficacy of EGCG in a APPswe/PS1dE9 Alzheimer's disease mice model, J. Contr. Release 301 (2019) 62–75.
[27] P. Luo, F. Wang, N.-K. Wong, Y. Lv, X. Li, M. Li, G.L. Tipoe, K.-F. So, A. Xu, S. Chen, Divergent roles of Kupffer cell TLR2/3 signaling in alcoholic liver disease and the protective role of EGCG, Cellular. Molecular Gastroenterology, Hepatology 9 (1) (2020) 145–160.
[28] Y. Zagury, S. Chen, R. Edelman, E. Karnieli, Y.D. Livney, β-Lactoglobulin delivery system for enhancing EGCG biological efficacy in HFD obesity mice model, J. Functional Foods 59 (2019) 362–370.
[29] K. Eun Lee, S. Bharadwaj, U. Yadava, S. Gu Kang, Evaluation of caffeine as inhibitor against collagenase, elastase and tyrosinase using in silico and in vitro approach, J. Enzyme Inhibition. Medicinal Chem 34 (1) (2019) 927–936.
[30] M.J. Moreno-Vásquez, E.L. Valenzuela-Buitimea, M. Plascencia-Jatomea, J.C. Encinas-Encinas, F. Rodríguez-Félix, S. Sánchez-Valdes, E.C. Rosas-Burgos, V.M. Ocaño-Higuera, A.Z. Graciano-Verdugo, Functionalization of chitosan by a free radical reaction: characterization, antioxidant and antibacterial potential, Carbohydr. Polym. 155 (2017) 117–127.
[31] R. Hlushko, J.F. Ankner, S.A. Sukhishvili, Layer-by-Layer hydrogen-bonded antioxidant films of linear synthetic polyphenols, Macromolecules 53 (3) (2020) 1033–1042.
[32] H. Liang, Y. Pei, J. Li, W. Xiong, Y. He, S. Liu, Y. Li, B. Li, pH-Degradable antioxidant nanoparticles based on hydrogen-bonded tannic acid assembly, RSC Adv. 6 (37) (2016) 31374–31385.
[33] Z. Lu, J. Gao, Q. He, J. Wu, D. Liang, H. Yang, R. Chen, Enhanced antibacterial and wound healing activities of microporous chitosan-Ag/ZnO composite dressing, Carbohydr. Polym. 156 (2017) 460–469.
[34] H. Chen, X. Xing, H. Tan, Y. Jia, T. Zhou, Y. Chen, Z. Ling, X. Hu, Covalently antibacterial alginate-chitosan hydrogel dressing integrated gelatin microspheres containing tetracycline hydrochloride for wound healing, Mater. Sci. Eng. C 70 (2017) 287–295.
[35] E.I. Rabea, M.E.-T. Badawy, C.V. Stevens, G. Smagghe, W. Steurbaut, Chitosan as antimicrobial agent: applications and mode of action, Biomacromolecules 4 (6) (2003) 1457–1465.
[36] M. Nikoo, J.M. Regenstein, H. Ahmadi Gavlighi, Antioxidant and antimicrobial activities of (-)-Epigallocatechin-3-gallate (EGCG) and its potential to preserve the quality and safety of foods, Compr. Rev. Food Sci. Food Saf. 17 (3) (2018) 732–753.
[37] G.L. Tipoe, T.-M. Leung, M.-W. Hung, M.-L. Fung, Green tea polyphenols as an anti-oxidant and anti-inflammatory agent for cardiovascular protection, Cardiovasc. Haematol. Disord. - Drug Targets 7 (2) (2007) 135–144.
[38] A. Novilla, D.S. Djamhuri, B. Nurhayati, D.D. Rihibiha, E. Afifah, W. Widowati, Anti-inflammatory properties of oolong tea (Camellia sinensis) ethanol extract and epigallocatechin gallate in LPS-induced RAW 264.7 cells, Asian Pacific J. Tropical Biomed 7 (11) (2017) 1005–1009.
[39] T. Hussain, B. Tan, Y. Yin, F. Blachier, M.C. Tossou, N. Rahu, Oxidative Stress and Inflammation: what Polyphenols Can Do for Us?, Oxidative Medicine and Cellular Longevity 2016, 2016.
[40] H. Zhang, R. Tsao, Dietary polyphenols, oxidative stress and antioxidant and anti-inflammatory effects, Current Opin. Food Science 8 (2016) 33–42.
[41] S.A. Al-Madhagy, N.M. Mostafa, F.S. Youssef, G.E. Awad, O.A. Eldahshan, A.N.B. Singab, Metabolic profiling of a polyphenolic-rich fraction of Coccinia grandis leaves using LC-ESI-MS/MS and in vivo validation of its antimicrobial and wound healing activities, Food. Function 10 (10) (2019) 6267–6275.
[42] G. Chen, L. He, P. Zhang, J. Zhang, X. Mei, D. Wang, Y. Zhang, X. Ren, Z. Chen, Encapsulation of green tea polyphenol nanospheres in PVA/alginate hydrogel for promoting wound healing of diabetic rats by regulating PI3K/AKT pathway, Mater. Sci. Eng. C 110 (2020) 110686.
[43] R. Jayakumar, M. Prabaharan, P.S. Kumar, S. Nair, H. Tamura, Biomaterials based on chitin and chitosan in wound dressing applications, Biotechnol. Adv. 29 (3) (2011) 322–337.
[44] E. Galun, J.H. Axelrod, The role of cytokines in liver failure and regeneration: potential new molecular therapies, Biochim. Biophys. Acta Mol. Cell Res. 1592 (3) (2002) 345–358.
[45] M.J. Cuevas, J. Tieppo, N.P. Marroni, M.J. Tuñón, J. González-Gallego, Suppression of amphiregulin/epidermal growth factor receptor signals contributes to the protective effects of quercetin in cirrhotic rats, J. Nutr. 141 (7) (2011) 1299–1305.
[46] N. Takagi, K. Kawakami, E. Kanno, H. Tanno, A. Takeda, K. Ishii, Y. Imai, Y. Iwakura, M. Tachi, IL-17A promotes neutrophilic inflammation and disturbs acute wound healing in skin, Exp. Dermatol. 26 (2) (2017) 137–144.
[47] A. Donato-Trancoso, A. Monte-Alto-Costa, B. Romana-Souza, Olive oil-induced reduction of oxidative damage and inflammation promotes wound healing of pressure ulcers in mice, J. Dermatol. Sci. 83 (1) (2016) 60–69.
[48] Y.H. Choi, I.H. Jang, S.C. Heo, J.H. Kim, N.S. Hwang, Biomedical therapy using synthetic WKYMVm hexapeptide, Organogenesis 12 (2) (2016) 53–60.
[49] R. Li, S. Lin, M. Zhu, Y. Deng, X. Chen, K. Wei, J. Xu, G. Li, L. Bian, Synthetic presentation of noncanonical Wnt5a motif promotes mechanosensing-dependent differentiation of stem cells and regeneration, Science Advanc 5 (10) (2019), eaaw3896.
[50] Q. Feng, S. Lin, K. Zhang, C. Dong, T. Wu, H. Huang, X. Yan, L. Zhang, G. Li, L. Bian, Sulfated hyaluronic acid hydrogels with retarded degradation and enhanced growth factor retention promote hMSC chondrogenesis and articular cartilage integrity with reduced hypertrophy, Acta Biomater. 53 (2017) 329–342.
[51] L. Bian, M. Guvendiren, R.L. Mauck, J.A. Burdick, Hydrogels that mimic developmentally relevant matrix and N-cadherin interactions enhance MSC chondrogenesis, Proc. Natl. Acad. Sci. Unit. States Am. 110 (25) (2013) 10117–10122.